

RSC Advances



This is an *Accepted Manuscript*, which has been through the Royal Society of Chemistry peer review process and has been accepted for publication.

Accepted Manuscripts are published online shortly after acceptance, before technical editing, formatting and proof reading. Using this free service, authors can make their results available to the community, in citable form, before we publish the edited article. This *Accepted Manuscript* will be replaced by the edited, formatted and paginated article as soon as this is available.

You can find more information about *Accepted Manuscripts* in the [Information for Authors](#).

Please note that technical editing may introduce minor changes to the text and/or graphics, which may alter content. The journal's standard [Terms & Conditions](#) and the [Ethical guidelines](#) still apply. In no event shall the Royal Society of Chemistry be held responsible for any errors or omissions in this *Accepted Manuscript* or any consequences arising from the use of any information it contains.



Journal Name

ARTICLE

PEI-Folic acid modified carbon nanodots for cancer cell-targeted delivery and two-photon excitation imaging

Received 00th January 20xx,

Accepted 00th January 20xx

DOI: 10.1039/x0xx00000x

www.rsc.org/

Jing Wang^{a*} Jun Liu^{a,b*}

Polyethyleneimine conjugated folic acid (PEI-FA) was coated onto the surfaces of fluorescent carbon nanodots (CDots) under neutral conditions through electrostatic interactions between the partially charged amino groups of PEI-FA and the carboxyl (-COOH) groups of the CDots surfaces. Because of the high abundance of folate receptors (FR) in cancer cells, folic acid (FA) was used as the targeting ligand to enhance the CDots' binding capability and penetration into the target cancer cells. We evaluated the amount of particles internalized by cancer cell lines displaying various levels of folate receptors. Two-photon excitation microscopy images revealed that the uptake of CDot-PEI-FA by FR-positive KB cancer cells was much higher than that by FR-negative A549 cancer cells. Moreover, quantitative flow cytometry analysis confirmed the receptor-mediated targeted delivery of the nanoparticles into different FR-expressing cells. The internalization of particles was ten-fold higher in the FR-positive KB cancer cells compared to that in the FR-negative A549 cancer cells; the difference was significant enough to be of biological importance. These preliminary results demonstrate the promising potential of CDot-PEI-FA for FR-positive cancer cell line diagnosis.

Introduction

Cancer remains a major public health issue around the world, generating increasing concern year after year.¹ Early diagnosis is critical for the detection, treatment, and monitoring of cancer.² In this respect, conventional methods such as computed tomography, magnetic resonance imaging, and radionuclide imaging play a key role, even if mainly suited for mature tissues.³ Nevertheless, the progress in optical imaging may engender new diagnostic methods for the early diagnosis of cancer, through the enhancement of sensitivity and spatiotemporal resolution.⁴ Many multicolour emissive materials have been developed for optical imaging in the past decades, such as semiconductor quantum dots (QDs),^{5,6} gold nanoparticles,^{7,8} rare-earth based nanoparticles,^{9,10} and organic fluorescence dyes,¹¹ but their potentially high toxicity, poor water solubility, low-emission quantum yields (QYs), or photobleaching properties have hampered their applications in biomedical.^{12,13} In 2006, along with the development of efficient surface modification methods, carbon nanodots (CDots) were opportunely recognized as

good water-soluble fluorescence agents.¹⁴ These CDots soon attracted a lot of interest in biomedical studies,^{15,16} due to their low toxicity features and consequently, higher biocompatibility potential.^{17,18} This new class of nanomaterials is considered to be a potential alternative to semiconductor QDs. Due to their high aqueous solubility, robust chemical inertness, easy functionalization, promising luminescence properties and non-blinking fluorescent emission,^{19,20} CDots have become a rising star in biomedical application development.²¹ Moreover, a few studies have described the use of CDots with large TPACS (two-photon absorption cross section) towards two-photon imaging.²²

Folate receptors (FR) are known to be upregulated in a variety of human cancerous cells, including ovarian, endometrial, colorectal, breast, lung, renal, and neuroendocrine carcinomas.²³ However, in normal cells, FR is only scarcely represented.²⁴ Therefore, the targeting of cancer cells through FR detection has attracted increasing interest. For FR, folic acid (FA) is an ideal ligand because of its high affinity ($K_d \approx 10^{-10}$ M), stability, and compatibility with both organic and aqueous solvents.²⁵ In this work, we strategically designed a novel CDot-conjugated PEI-FA in order to achieve higher specificity. FA serves as the targeting ligand, leading to a selective internalization of the nanoparticles within FR-positive cancer cells. Surfaces of CDots covered with PEI prevent absorption of plasma proteins, thereby increasing the particle blood circulation time and allowing the nanoparticles to reach their target tissues. In order to study the delivery of CDots-PEI-FA to targeted cancer cells, KB cell lines (human nasopharyngeal epidermal carcinoma cell lines), with significantly high folic acid receptor expression, and A-549 cell lines (human lung epithelial carcinoma cancer cell lines), with low folic acid receptor expression, were chosen as the positive and negative

^a State Key Laboratory of High Field Laser Physics, Shanghai Institute of Optics and Fine Mechanics, Chinese Academy of Sciences, Shanghai 201800, People's Republic of China.

^b Collaborative Innovation Center of IFSA (CICIFSA), Shanghai Jiao Tong University, Shanghai 200240, China.

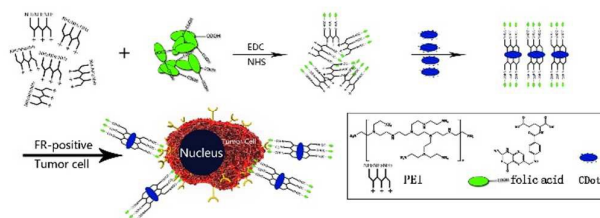
† Footnotes relating to the title and/or authors should appear here.

Electronic Supplementary Information (ESI) available: [details of any supplementary information available should be included here]. See DOI: 10.1039/x0xx00000x

control models, respectively. Because the absorption and scattering of light by live tissues are much lower for NIR light than for visible light, we used a near infrared laser to conduct the two-photon excitation imaging (TPE) and treat deeper cancers. First, we measured TPACS of aqueous CDots in the 700–800 nm region. The large TPACS obtained confirmed their suitability for TPE imaging. The microscopy images revealed that the nanocomposites were readily internalized into FR-positive cells through receptor mediated endocytosis to a much higher extent than they were in FR-negative cells. The quantitative flow cytometry experiments further confirmed this result.

Results and discussion

Development of selective and sensitive methods to distinguish cancer cells from normal cells is of great importance for tumour diagnosis and therapy. In this study, we aimed to detect cancer cells overexpressing the folate receptor (FR) in vitro by using folic acid (FA) coated carbon nanodots (CDots) as the targeting fluorescence imaging probe agents. The design of this experimental work is shown in Scheme 1.



Scheme 1. Synthesis and targeting of CDot-PEI-FA conjugates for two-photon excitation imaging of cancer cells. The diagram is not drawn to scale.

Based on transmission electron microscopy (TEM) imaging (Fig. 1A), we observed that the prepared CDots were relatively uniform in size with an average diameter of 8 nm. A Fourier transform infrared (FTIR) spectrum (Fig. 1B) confirmed the presence of NH_2 , OH, COOH, and SH groups on the surface of the CDots. There were three bands at 1570, 1510, and 1450 cm^{-1} , attributed to the C=C stretching mode of the polycyclic aromatic hydrocarbons. The peaks observed at 3050–3400 cm^{-1} and at 1710 cm^{-1} were assigned to =N-H/O-H/C-H and C=O/COOH stretching vibrations, respectively. Moreover, a strong and broad band at 1200–1300 cm^{-1} , corresponding to the C-O/C-N/C-C asymmetric stretching vibrations, suggested that the CDots surfaces contained both -COOH and -OH groups.^{26,27} Therefore, we can consider that the CDots are negatively charged in neutral solution. After PEI-FA coating, the TEM images of the CDot-PEI-FA nanocomposites showed good dispersion in spite of an increase in their average diameter up to 10 nm (Fig. 1C). High-resolution transmission electron microscopy (HRTEM) showed that the surfaces of CDots were coated with a layer (pointed out by the arrow), indicating the presence of PEI-FA in the complexes (Fig. 1D).

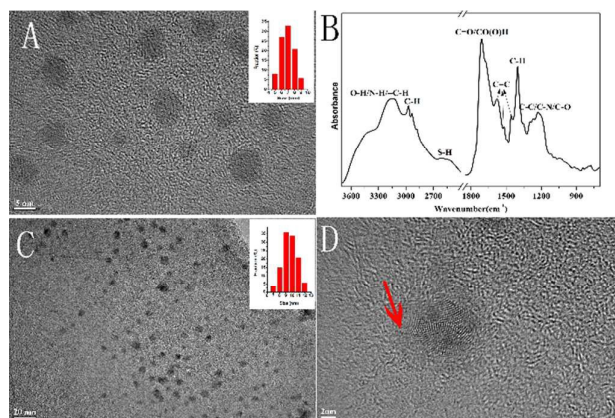


Fig. 1 (A) TEM image of CDots before coating with PEI-FA. The inset in A) presents the distribution of the diameters of the CDots. (B) FTIR spectrum of CDots. (C) TEM image of CDots coated with PEI-FA. The inset in C) presents the diameters' distribution of CDot-PEI-FA. (D) HRTEM images of a CDot-PEI-FA.

In order to form the PEI-FA complex, folic acid (FA) was conjugated to polyethyleneimine (PEI, 600 Da) through the creation of a hydrogen bond between the carboxylic groups of FA and primary amine groups of PEI with the help of 1-ethyl-3-(3-dimethylaminopropyl)carbodiimide (EDC) and N-hydroxysuccinimide (NHS), which led to the formation of PEI-FA. The carboxyl groups situated on the surfaces of the CDots display negative charges generating an electrostatic attraction with the positively charged PEI-FA.

For a selected CDot concentration (10 mg/mL), various mass ratios of CDots to PEI-FA were tested in order to find the optimal conjugation conditions. The reversed zeta-potential value of the CDot-PEI-FA complexes indicated successful coating of PEI-FA onto the CDot surfaces (Fig. 2A). Upon increasing the PEI-FA amount, the CDot-PEI-FA complexes showed an increase in positive zeta potential values accordingly, suggesting the accumulation of PEI-FA on the CDots surfaces. Finally, a mass ratio of 10 mg/mL (CDots) to 10 mg/mL (PEI-FA) was selected for conjugation, as this ratio allowed the CDots to be almost totally coated with PEI-FA. When adding more PEI-FA, the Zeta potential of the CDot-PEI-FA did not increase any further. The PEI-FA conjugate can easily be dissolved in deionized water, resulting in a peak around $\lambda = 280\text{--}370$ nm in the UV/Vis spectrum that is characteristic to the FA molecule.^{28,29} After PEI-FA coating, the CDot-PEI-FA complexes showed a UV/Vis absorbance peak at $\lambda = 280$ nm, indicating the presence of FA molecules within the complexes (Fig. 2B).³⁰ In addition, the sizes of the CDots increased after conjugation with PEI-FA (Fig. 1D), confirming the success of the surface coating with PEI-FA. We tested the fluorescence intensity of CDots before and after coating with PEI-FA. The fluorescence intensity of the CDot-PEI-FA (1:1) decreased by 18%, compared with the same concentration of CDots alone (Fig. 2C). We then measured the absorption spectrum of the freshly prepared CDots and CDot-PEI-FA as well as their three month-old counterparts (Fig. 2D). The overlapping spectra demonstrated their good stability.

When using probes in living systems, toxicity is of great concern. The cytotoxicity of CDot-PEI-FA was evaluated with the 3-(4,5-dimethylthiazol-2-yl)-2,5-diphenyltetrazolium bromide (MTT)

assay. The viability of KB cells was measured following incubation with increasing CDot-PEI-FA concentrations for 24 h. As shown in Fig. 2E, CDot-PEI-FA was hypotoxic. When the concentration of CDot-PEI-FA increased to 250 mg mL^{-1} , the KB cells survival rate remained above 85%. Similar results were observed with HeLa cells (Fig. 2F). Taking into account the fact that the incubation time of CDot-PEI-FA in this experiment was 24 h while the incubation time of CDot-PEI-FA in the cell staining experiments was only 30 min, we considered that the cytotoxicity of CDot-PEI-FA could be neglected.

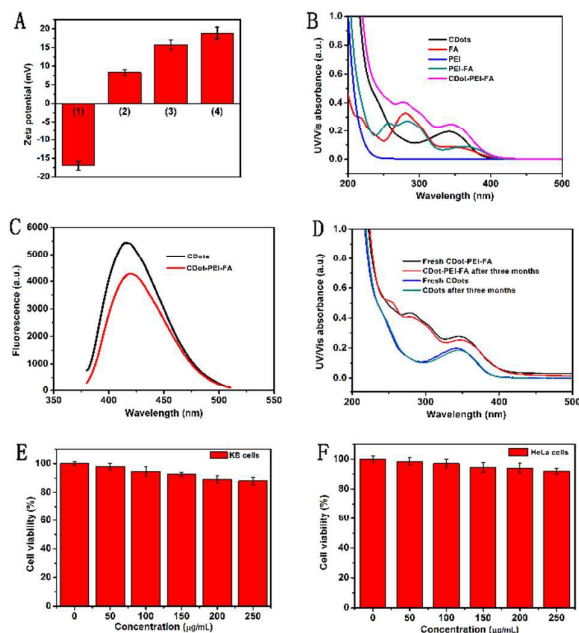


Fig. 2 (A) Zeta-potential measurements (1) CDots, (2) CDot-PEI-FA (1:0.5), (3) CDot-PEI-FA (1:1), (4) CDot-PEI-FA (1:4) indicate the CDots to PEI-FA coating ratio. All samples were dissolved or resuspended in deionized water. (B) UV/Vis spectra. (C) The fluorescence intensity of CDots before and after 1:1 coating with PEI-FA. (D) Absorbance spectra. (E) KB Cell viability (%) measured by MTT assay. The KB and HeLa cells were incubated with the CDot-PEI-FA (10 mg/mL) for 1 h and then incubated 24 h at 37°C . All results were presented as the mean \pm standard deviation (SD) from three independent experiments, using four wells in each.

In order to analyse the CDot-PEI-FA compound with TPE imaging, we first studied the TPACS of the CDots. Several research teams have reported that CDots had high TPACS, however, all of them only measured the TPACS of CDots at 800 and 810 nm.³¹ From the UV/Vis absorption spectrum of CDots (Fig. 2B), we can see that CDots have an absorption peak at 350 nm and therefore the maximum TPACS of CDots should emerge around 700 nm. We consequently measured TPACS of CDots in aqueous solution with femtosecond (fs) laser induced TPE fluorescence readings at wavelengths comprised between 700 nm and 800 nm. As shown in Fig. 3A, the TPE induced fluorescence of CDots greatly depends on the excitation wavelength. The inset of Fig. 3A illustrates that the bright blue fluorescence generated by CDots can be clearly seen with naked eyes within the light path of the 800 nm fs laser. The TPACS of CDots at different excitation wavelengths were measured using Rhodamine B as a reference sample (Fig. 3C). We evaluated the

relationship between the fluorescence intensity of CDots and excitation power of the fs laser. As shown in Fig. 3B, the linear dependence between fluorescence intensity and excitation power confirmed the validity of the TPE process. The important finding arising from this experiment resides in TPACS of CDots being 10 fold higher at 700 nm than 800 nm. This is the first report of this phenomenon to our knowledge, offering a clear opportunity to enhance TPE applications of CDots.

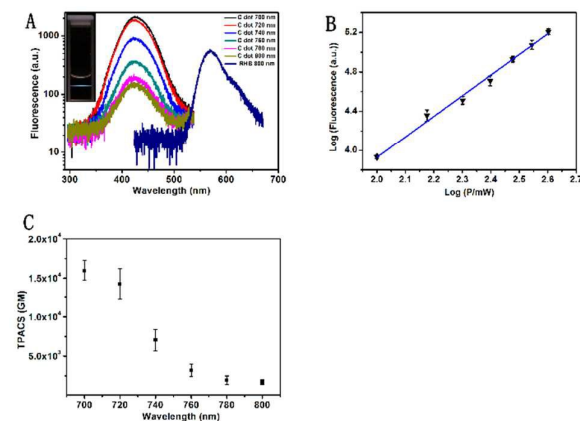


Fig. 3(A) Logarithmic plots of the TPE induced fluorescence emission spectra of Rhodamine B (20 mM) and CDots (1.16 mM) at different excitation wavelengths with a 400 mW fs laser. The inset picture in (A) represents the CDots fluorescence in the laser beam's path. (B) Logarithmic plots showing the dependence between relative TPE induced fluorescence of CDots and the irradiation power of an fs laser at 700 nm . The fitted slope is 2.07. The estimated uncertainty of the fitted slope is ± 0.1 . (C) TPACS of the CDot at selected wavelengths.

Confocal microscopic imaging has emerged as a promising technique for the detection, diagnosis, and stage estimation of cancer. In this work, the application of CDot-PEI-FA complex in two-photon exciting microscopy improves the detection and characterization of lesions by enhancing the signal intensity of the target tissues. As shown in Fig. 4, the fluorescence images of CDot-PEI-FA incubated KB cells were bright, unlike the CDots incubated KB cells which displayed a weak signal. The results demonstrate that a much higher number of CDot-PEI-FA entered KB cells compared to CDots alone, reflecting an enhanced recognition and binding ability of CDot-PEI-FA towards KB cells. In order to check whether the CDot-PEI-FA had specific affinity to FR-positive cancer cells, the binding of CDot-PEI-FA to FR-negative A549 cells was tested under the same conditions. After a 30-min incubation of CDot-PEI-FA ($10 \text{ }\mu\text{g/mL}$), the fluorescence image (Fig. 4C) of A549 cells was acquired. The dim image of A549 cells obtained, in contrast with KB cells (Fig. 4A), shows that the binding efficiency of CDot-PEI-FA to the FR negative A549 cells was lower than FR positive KB cells. Further experimental work was performed in order to assess whether the association of CDot-PEI-FA with KB cells was mediated by FR. Supposing that the FR proteins on the surfaces of KB cells are fully occupied by free FA, the association of CDot-PEI-FA should hence be blocked. We thus pre-treated KB cells with excess free FA (20 mM) for 1 h, and subsequently incubated these cells with CDot-PEI-FA ($10 \text{ }\mu\text{g/mL}$) for 30 min. The relatively weak fluorescence image obtained (Fig. 4D) from these double-treated

cells suggests that the association of CDot-PEI-FA with KB cells was indeed mediated by the binding of the FA terminal with their surface FR. These results show that the CDot-PEI-FA can effectively target FR positive cancer cells via an FR mediated process.

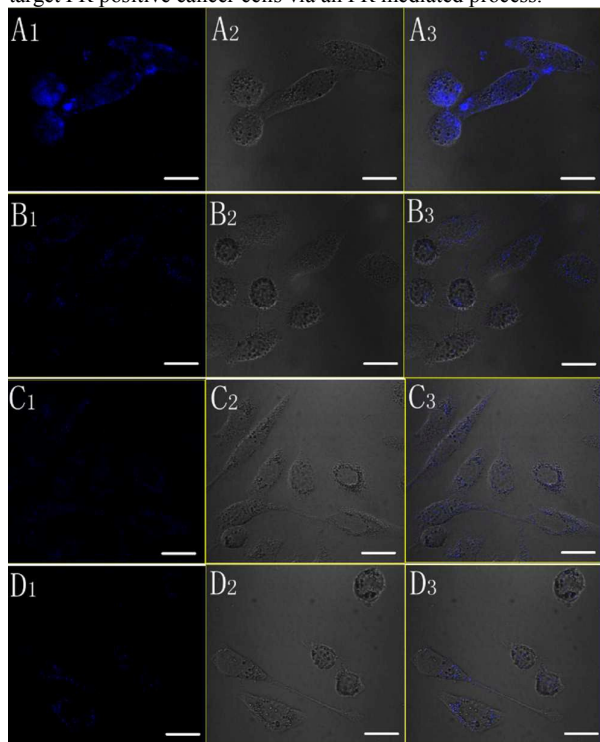


Fig. 4 Fluorescence images of intracellular nanocomposites in KB cells and A549 cells under 700 nm TPE. Blue colour is the fluorescence of the CDots. Left: fluorescence images, middle: DIC images, right: the merged images. (A) KB cells have been incubated with CDot-PEI-FA (10 $\mu\text{g}/\text{mL}$) for 30 min; (B) KB cells have been incubated with CDots (10 $\mu\text{g}/\text{mL}$) for 30 min; (C) A549 cells have been incubated with CDot-PEI-FA (10 $\mu\text{g}/\text{mL}$) for 30 min; (D) KB cells were treated 1 h with excess FA (20 mM) and then incubated with CDot-PEI-FA (10 $\mu\text{g}/\text{mL}$) for 30 min.

It should be noted that the comparison of luminescence intensities from laser scanning microscopy imaging only allows a qualitative analysis whereas a quantitative analysis of the luminescence intensity can be performed using flow cytometry. From Fig. 5A, we can see, upon excitation at $\lambda = 355$ nm, KB cells incubated with CDot-PEI-FA (10 $\mu\text{g}/\text{mL}$) at 37 $^{\circ}\text{C}$ for 30 min, displaying much higher emission intensities than those incubated with the same amount of CDots and CDot-PEI, in the same conditions. This clearly indicates that CDot-PEI-FA nanocomposites had a higher ability to target FR-positively KB cells. We prepared these CDot-PEI (deprived of the FA terminal group) in order to experimentally confirm the importance of the FA terminal in the recognition and binding process. The KB cells showed enhanced fluorescence when incubated with CDot-PEI compared with that when they were incubated with CDots only. As CDot-PEIs carry a highly positive surface charge under the studied conditions, electrostatic attraction of the particles to the negatively charged cell membrane could explain this phenomenon. To confirm the ability of CDot-PEI-FA particles to specifically target KB cells, we compared the uptake of the nanocomposites by both KB and A-549 cells under identical

conditions. When comparing Fig. 5A with 5B we observe that the uptake of the CDot-PEI-FA by KB cells, after 30 min incubation, is more than 10-fold higher than for A-549 cells, according to our flow cytometry results (Fig. 5). Moreover, the cells from both controls display scarce fluorescence. When the A-549 cells were treated with either CDot-PEI-FA or CDot-PEI, similar fluorescence intensities were observed, probably because the transfection efficiency of CDot-PEI-FA in FR-negative A-549 cells was not influenced by the terminal FA.

Those results confirm that the observed fluorescence in KB cells was indeed generated by the receptor-mediated endocytosis of CDot-PEI-FA.

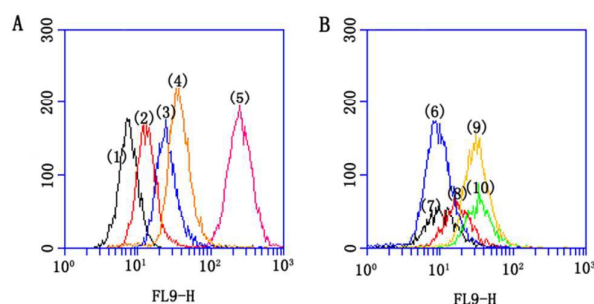


Fig. 5 Flow cytometry profiles of cellular uptake of CDot-PEI-FA in KB cells (A) and A549 cells (B). A(1) control (no treatment); A(2) treated for 1 h with excess FA (20 mM) and then incubated with CDot-PEI-FA (10 $\mu\text{g}/\text{mL}$) for 30 min; A(3) CDots (10 $\mu\text{g}/\text{mL}$) incubated for 30 min; A(4) CDot-PEI (10 $\mu\text{g}/\text{mL}$) incubated for 30 min; A(5) CDot-PEI-FA (10 $\mu\text{g}/\text{mL}$) incubated for 30 min; B(6) control (no treatment); B(7) treated for 1 h with excess FA (20 mM) and then incubated with CDot-PEI-FA (10 $\mu\text{g}/\text{mL}$) for 30 min; B(8) CDots (10 $\mu\text{g}/\text{mL}$) incubated for 30 min; B(9) CDot-PEI (10 $\mu\text{g}/\text{mL}$) incubated for 30 min; B(10) CDot-PEI-FA (10 $\mu\text{g}/\text{mL}$) incubated for 30 min; X axis: log fluorescence intensity; Y axis: cell number.

Experimental

2.1 Materials and devices

Polyethylenimine (PEI) (600 Da) was obtained from Aladdin and used as received. 1-ethyl-3-[3-dimethylaminopropyl]-carbodiimide hydrochloride (EDC), N-hydroxysuccinimide (NHS), folic acid (FA) and DMSO were purchased from Sigma-Aldrich and used as received. Dulbecco's modified eagle medium (DMEM), foetal bovine serum, penicillin (100 $\mu\text{g mL}^{-1}$), streptomycin (100 $\mu\text{g mL}^{-1}$) and phosphate buffered saline (PBS) solution were obtained from Invitrogen Co. KB cells (human nasopharyngeal epidermal carcinoma cell lines) and A549 cells (human lung epithelial carcinoma cancer cell lines) were obtained from the Shanghai Science Academy cell bank.

The size of the CDots was determined by a TEM instrument at 200 kV (JEOL JEM-2010F). The UV-Vis spectra were recorded in 1 cm quartz cells with a Hitachi U-500 absorption spectrophotometer (Tokyo, Japan). Fourier transform infrared (FTIR) spectra of CDots were obtained using an IRPRESTIGE-21 spectroscope (Shimadzu) with KB pellets. The zeta potentials were measured in water using a Malvern Zetasizer (ZEN 3600, Worcestershire, UK).

2.2 Synthesis of the CDots

The CDots were prepared using a well-established hydrothermal treatment previously described.³² Briefly, citric acid monohydrate (2 g, 9.5 mmol) and L-cysteine (1 g, 8.3 mmol) were dissolved in water (5 mL), followed by drying at 70°C overnight. Then, the pale yellow syrup was re-dispersed in water (25 mL) and heated hydrothermally in a Teflon-equipped stainless-steel autoclave at 200°C for 6 h.

2.3 TPE spectral measurement of CDots

A high-performance mode-locked Ti:sapphire laser (Spectra Physics Mai Tai eHP) of 100 fs pulse width and 80 MHz repetition rate was used for two-photon excitation (TPE). The wavelength of the output laser beam could be tuned from 690 to 1040 nm. We focused the laser beam with a 350 mm focal length lens onto a cuvette containing the sample solution. The focal spot was about 200 μm in diameter. The induced fluorescence was directed onto the entrance slit of a spectrometer (Acton, Spectropro 2150i). The fluorescence spectra were recorded by a liquid nitrogen-cooled CCD (Princeton, Spec-10:100B LN) that was mounted onto the spectrometer.

2.4 TPACS measurements of CDots

The two-photon absorption cross section (TPACS) of CDots was measured by comparing the TPE induced fluorescence of CDots against that of reference Rhodamine B. The relationship of the CDots photoluminescence (PL) with related parameters under TPE is detailed in the following formula (1)³³

$$F = K\Phi CL\delta I^2 / 2 \quad (1)$$

Where δ is the two-photon absorption cross section (TPACS), I is the flux of incident photons (photons/cm²s), Φ is the PL quantum yield, and the F is the integrated PL of the sample under TPE. C is the fluorophore density (sample concentration), L is the length of the path within which photons are absorbed, and K is a constant parameter specific to the instrument. Since the TPACS of the reference Rhodamine (δ_r) has been determined as 210 GM (1 GM = 10⁻⁵⁰ cm⁴ s/photon),³⁴ δ of the CDots can be expressed in function of δ_r and other parameters in formula (2)

$$\delta = \frac{F}{F_r} \frac{\Phi_r C_r}{\Phi C} \delta_r \quad (2)$$

2.5 Preparation of CDot-PEI-FA

Folic acid (100 mg) was dissolved in DMSO (5 mL). Then, DMSO (5 mL) containing EDC (70 mg) and NHS (200 mg) were added into the folic acid solution. The solution was incubated in the dark and stirred for 2 h before an aqueous solution (20 mL) containing PEI (800 mg) was added. Then, the pH value of the solution was adjusted to 8 by adding a proper amount of an aqueous solution of NaOH (0.2 M). The mixture was kept stirring for three days, and then dialysis against deionized H₂O was performed in a dialysis membrane (1 K) for five days in order to remove excess folic acid and by-products. The PEI-FA conjugate was collected by freeze-drying. Then, PEI-FA (1 mg) and CDot (1 mg) were added into deionized H₂O (1 mL), which was stirred for another half a day. PEI-FA coated CDots were collected. The CDot-PEI complex was prepared by directly incubating the CDot (1 mg) with PEI (1 mg) into deionized H₂O (1 mL) and stirred for half a day.

2.6 Cell culture and cell treatments with CDots-PEI-FA

KB cells (human nasopharyngeal epidermal carcinoma cell lines) and A549 cells (human lung epithelial carcinoma cancer cell lines) were obtained from the Shanghai Science Academy cell bank. The cells were seeded in culture dishes containing DMEM medium with 10% calf serum, 100 units mL⁻¹ penicillin, 100 μg mL⁻¹ streptomycin and 100 μg mL⁻¹ neomycin, and then incubated in a humidified incubator at 37°C with 5% CO₂. When the cells reached 80% confluence with normal morphology, the compound was added and the cell dish was placed in the incubator for the desired time. After incubation, the cells were washed three times with PBS to remove un-associated compounds, and used for further experiments.

2.7 Cytotoxicity assay experiments

3-(4,5-dimethylthiazol-2-yl)-2,5-diphenyltetrazolium bromide (MTT) was used to measure the cytotoxicity effect of CDot-PEI-FA on the KB cancer cell line. The cells, at a concentration of 3 × 10⁴ cells/mL were seeded in each well of a 96-well flat bottom tissue culture plate and allowed to attach overnight. The CDot-PEI-FA was added to the wells at increasing concentrations of 50, 100, 150, 200, and 250 mg/mL. Cells were incubated for 24 h at 37 °C before adding 10 mL of MTT solution (5 mg/mL) and incubating for 1.5 h. Finally, the optical densities (O.D) at 450 nm were measured in each well using an iEMSA Analyzer (Lab-system). The cell viability in each well was determined by comparing its O.D value with of the ones obtained for untreated control cells contained within the same plate. All results were presented as the mean ± SE from three independent experiments (n = 4 wells each).

2.8 Imaging measurements of CDot-PEI-FA in cells by the TPE

TPE fluorescence imaging of cells was performed using a Olympus FV-1000 laser scanning microscope, coupled with a high-performance mode-locked Ti:sapphire laser (Spectra Physics Mai Tai eHP). The TPE fluorescence images of CDots-PEI-FA in cells were collected through a water immersion objective (60×, 1.2 N.A.) with a band-pass filter of 360–450 in detection channel 1. The excitation laser power on the cells was about 5 mW (62.5 pJ/pulse), as measured with a power meter (Newport, Model No. 1918-C).

2.9 The cellular uptake of CDots-PEI-FA measured with flow-cytometric analysis

To evaluate the cellular uptakes of CDot-PEI-FA between the difference cell lines in a large number of cells, flow-cytometry analysis was performed using a BD influx flow cytometer. Cells (about 10⁶ cells in a 35-mm culture dish) incubated with CDot-PEI-FA for 30 min were washed three times with PBS to remove the unbound CDot-PEI-FA and were trypsinized using 0.25% trypsin-EDTA. The cell suspension was then ready for flow-cytometry analysis. A 355 nm laser was used to excite CDot-PEI-FA in each passing flow cell and FL-9 channel (405–450 nm) was used to detect CDot-PEI-FA emissions from a train of flowing cells. A minimum of 3000 cells per group were analysed.

Conclusions

In summary, we have successfully fabricated carbon nanodots displaying PEI-FA, which were capable of both targeting and entering cancer cells. The cancer-targeting property of the nanoconjugates through folic acid receptor mediated endocytosis

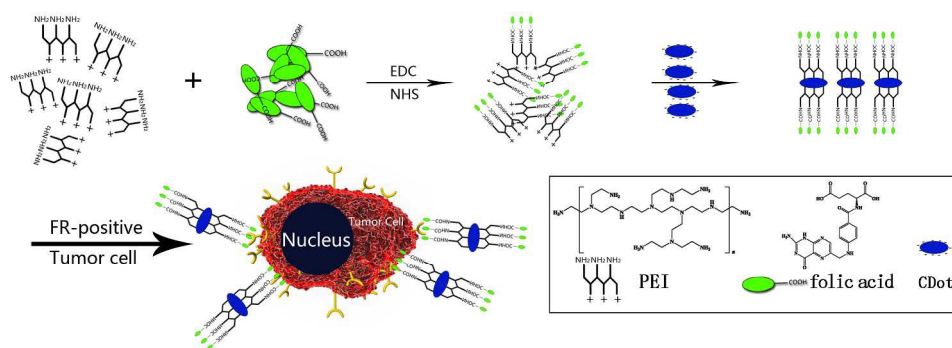
has been demonstrated using KB cells (FA positive receptor) and A-549 cells (FA negative receptor). The results of two-photon excitation microscopy imaging and flow cytometry studies demonstrated that CDot-PEI-FA could target tumour cells possessing large numbers of folate receptors. This current research paves the way towards the development of novel co-delivery systems and improved therapy of cancer.

Acknowledgements

This work is supported by the National Natural Science Foundation of China (NSFC) (grants 61178006, 11274327, 61221064 and 61527821) and the Recruitment Program of Global Youth Experts.

References

- D. M. Parkin, *Lancet Oncol.* 2001, 2, 533-543.
- J. F. Rusling, C. V. Kumar, J. S. Gutkind and V. Patel, *Analyst* 2010, 135, 2496-2511.
- K. Yan, P. Li, H. Zhu, Y. Zhou, J. Ding, J. Shen, Z. Li, Z. Xu and P. K. Chu, *RSC Advances*, 2013, 3, 10598-10618.
- W. Zhang, J. Ye, Y. Zhang, Q. Li, X. Dong, H. Jiang and X. Wang, *RSC Advances*, 2015, 5, 63821-63826.
- D. J. Bharali, D. W. Lucey, H. Jayakumar, H. E. Pudavar and P. N. Prasad, *J. Am. Chem. Soc.* 2005, 127, 11364-11371.
- S. Kim, Y. T. Lim, E. G. Soltesz, A. M. De Grand, J. Lee, A. Nakayama, J. A. Parker, T. Mihaljevic, R. G. Laurence, D. M. Dor, L. H. Cohn, M. G. Bawendi and J. V. Frangioni, *Nat. Biotechnol.* 2004, 22, 93-97.
- L. Minati, V. Antonini, L. Dalbosco, F. Benetti, C. Migliaresi, M. Dalla Serra, and G. Speranza, *RSC Advances*, 2015, 5, 103343-103349.
- H. Alisafae, J. Marmon, and M. A. Fiddy, *Photonics Research*, 2014, 2, 10-14.
- H. Isshiki, F. Jing, T. Sato, T. Nakajima, and T. Kimura, *Photonics Research*, 2014, 2, A45-A55.
- Z. Zhang, X. Ma, Z. Geng, K. Wang and Z. Wang, *RSC Advances*, 2015, 5, 33999-34007.
- U. Resch-Genger, M. Grabolle, S. Cavaliere-Jaricot, R. Nitschke and T. Nann, *Nat. methods*, 2008, 5, 763-775.
- A. M. Derfus, W. C. W. Chan and S. N. Bhatia, *Nano Lett.* 2004, 4, 11-18.
- M. De, P. S. Ghosh and V. M. Rotello, *Adv. Mater.* 2008, 20, 4225-4241.
- Y. P. Sun, B. Zhou, Y. Lin, W. Wang, K. S. Fernando, P. Pathak, et al. *J. Am. Chem. Soc.* 2006, 128, 7756-7757.
- S. T. Yang, L. Cao, P. G. Luo, F. Lu, X. Wang, H. Wang, et al. *J. Am. Chem. Soc.* 2009, 131, 11308-11309.
- P. G. Luo, S. Sahu, S. T. Yang, S. K. Sonkar, J. Wang, H. Wang, G. E. LeCroy, L. Cao, Y. P. Sun, *J. Mater. Chem. B* 2013, 1, 2116-2127.
- M. Shim, N. W. Shi Kam, R. J. Chen, Y. Li, H. J. Dai, *Nano Lett.* 2002, 2, 285-288.
- S. T. Yan, X. Wang, H. Wang, F. Lu, P. G. Luo, L. Cao, et al. *J. Phys. Chem. C* 2009, 113, 18110-18114.
- H. Li, Z. Kang, Y. Liu, S. T. Lee, *J. Mater. Chem.* 2012, 22, 24230-24253.
- S. Zhu, Q. Meng, L. Wang, J. Zhang, Y. Song, H. Jin, et al. *Angew. Chem.* 2013, 125, 4045-4049.
- S. N. Baker, G. A. Baker, *Angew. Chem., Int. Ed.* 2010, 49, 6726-6744.
- J. Tang, B. Kong, H. Wu, M. Xu, Y. Wang, Y. Wang, et al. *Adv. Mater.* 2013, 25, 6569-6574.
- H. F. Dong, J. P. Lei, H. X. Ju, F. Zhi, H. Wang, W. J. Guo, Z. Zhu, F. Yan, *Angew. Chem., Int. Ed.* 2012, 51, 4607-4612.
- S. D. Weitman, R. H. Lark, L. R. Coney, D. W. Fort, V. Frasca, V. R. Zurawski, B. A. Kamen, *Cancer Res.* 1992, 52, 3396-3401.
- P. S. Low, and A. C. Antony, *Adv. drug delivery Rev.* 2004, 56, 1055-1058.
- F. Wang, S. Pang, L. Wang, Q. Li, M. Kreiter, and C. Y. Liu, *Chem. Mater.* 2010, 22, 4528-4530.
- H. Peng, and J. Travas-Sejdic, *Chem. Mater.* 2009, 21, 5563-5565.
- G. A. Mansoori, K. S. Brandenburg, and A. Shakeri-Zadeh, *Cancers* 2010, 2, 1911-1928.
- X. Ma, Y. Zhao, K. W. Ng, and Y. L. Zhao, *Chem. Eur. J.* 2013, 19, 15593-15603.
- L. Zhang, J. Xia, Q. Zhao, L. Liu, and Z. Zhang, *Small* 2010, 6, 537-544.
- A. Zhu, Z. Luo, C. Ding, B. Li, S. Zhou, R. Wang, and Y. A. Tian, *Analyst*, 2014, 139, 1945-1952.
- Y. Dong, H. Pang, H. B. Yang, C. Guo, J. Shao, Y. Chi, et al. *Angew. Chem., Int. Ed.* 2013, 52, 7800-7804.
- A. Fischer, C. Cremer, and E. H. K. Stelzer, *Appl. Opt.* 1995, 34, 1989-2003.
- C. Xu, and W. W. Webb, *J. Opt. Soc. Am. B* 1996, 13, 481-491.



995x361mm (72 x 72 DPI)